



SAKARYA ÜNİVERSİTESİ

FEN BİLİMLERİ ENSTİTÜSÜ DERGİSİ

Sakarya University Journal of Science
SAUJS

e-ISSN 2147-835X Period Bimonthly Founded 1997 Publisher Sakarya University
<http://www.saujs.sakarya.edu.tr/>

Title: Boost Converter Based 3-Phase AC-AC Active Tracking Voltage Regulator Controlled by a Robust Hybrid Control Method

Authors: Faruk YALÇIN, Felix HIMMELSTOSS

Received: 2021-06-14 00:00:00

Accepted: 2021-12-13 00:00:00

Article Type: Research Article

Volume: 26

Issue: 1

Month: February

Year: 2022

Pages: 24-37

How to cite

Faruk YALÇIN, Felix HIMMELSTOSS; (2022), Boost Converter Based 3-Phase AC-AC Active Tracking Voltage Regulator Controlled by a Robust Hybrid Control Method.

Sakarya University Journal of Science, 26(1), 24-37, DOI:

10.16984/saufenbilder.900421

Access link

<http://www.saujs.sakarya.edu.tr/tr/pub/issue/67934/900421>

New submission to SAUJS

<http://dergipark.gov.tr/journal/1115/submission/start>

Boost Converter Based 3-Phase AC-AC Active Tracking Voltage Regulator Controlled by a Robust Hybrid Control Method

Faruk YALÇIN*¹, Felix HIMMELSTOSS²

Abstract

In this study, a switch-mode three-phase active tracking AC-AC voltage regulator based on the boost converter is proposed with a moderate number of active and passive elements used in the topology. A robust hybrid control, where a novel designed feedforward controller supports the closed-loop PID controller, is proposed for the control of the regulator apart from similar studies in the literature. Active tracking response of the reference output phase voltages is augmented by the proposed hybrid control method. Thus nearly close to sine-wave output phase voltages can be obtained, whether the input AC phase voltages are ideal pure sine or not. Also, the modular structure of the regulator topology enables independent control for each output phase. Thus, the supply of balanced/unbalanced wye-connected three-phase loads or independent single-phase loads with nearly close to ideal sine wave voltages can be achieved by the modularity of the regulator. Both experimental and simulation test studies are performed for the proposed regulator system. A laboratory set-up for the regulator is designed for 0-200 V_p input phase voltages (50 Hz), and 0-300 V_p output phase voltages, and 1.8 kW output power. The achieved results for both simulation and experimental tests verify the proposed switch-mode boost-type regulator's ability to provide output phase voltages nearly close to sine wave with total harmonic distortion (THD) values under 5%.

Keywords: AC-AC regulator, active tracking, boost converter, three-phase, THD

1. INTRODUCTION

Distortion of power quality in power systems is continuously increased due to the increasing energy demand and this causes a major problem for AC loads. A required alternating voltage has to supply AC loads within a determined magnitude band, where some of the AC loads accept only a small band. Voltage sags or voltage swells occur due to the various operating

conditions, such as loading in the distribution network, that affect the power quality of the AC loads. Besides, some AC loads such as AC motors need to be supplied by adjustable voltages that differ from the grid voltage levels. Many studies and solutions are presented in the literature for AC voltage regulation.

FACTS (flexible ac transmission systems) devices are the main providers of voltage

* Corresponding author: farukyalcin@sakarya.edu.tr

¹ Sakarya University of Applied Sciences, Faculty of Technology, Department of Mechatronics Engineering, ORCID: <https://orcid.org/0000-0003-2672-216X>

² University of Applied Sciences Technikum Wien, Austria
E-Mail: felix.himmelstoss@technikum-wien.at
ORCID: <https://orcid.org/0000-0001-8482-2295>

regulation for voltage variations in distribution systems. For this aim, voltage sag supporters [1, 2], voltage sag/swell compensators [3, 4], DVRs (dynamic voltage restorers) [5, 6], and voltage conditioners [7, 8], are developed and applied successfully. The desired distribution network voltage is provided by these devices to the distribution buses where the AC loads are connected. Therefore, it is not possible to provide voltage regulation for the end-user AC loads independently by this method. However, these VSI (voltage source inverter) structured FACTS need a coupling transformer. VSIs may be designed as a DC-AC converter or an AC-DC-AC converter in these FACTS devices based regulators. Independent external DC storage systems such as capacitors or batteries are needed for the VSIs which are based on a DC-AC converter. Because of this, long duration accurate voltage sags/swells compensation cannot be obtained by using DC-AC converter-based VSIs. In addition, capacities of the external storage units limit the compensation capabilities. External storage systems are not needed in AC-DC-AC based converters as the AC-DC sub-units already exist. But the effect of additional increasing loss, caused by the AC-DC topology, is the main disadvantage of the AC-DC-AC converters.

In many applications only VSIs based on AC-DC-AC converters are chosen for voltage regulation for AC loads [9, 10]. By this way, the need for additional coupling transformers, as used in the FACTS-based regulators mentioned above, is eliminated. In addition, this method provides independent voltage regulation control of each AC load individually where the distribution voltage level is constant at the load buses. However, AC-DC stage before DC-AC stage of the AC-AC conversion structure brings additional loss. This is the mayor disadvantage of these VSIs.

AC-AC conversion emerges as the ideal solution in contrast to direct VSI applications and FACTS devices-based regulation systems, because FACTS-based or direct VSI-based techniques have large complexity and limited feature problems. In the literature, the researchers developed many kinds of AC-AC regulators. The

simplest and the traditional solution for direct AC-AC regulation can be provided by AC-AC PWM choppers [11]. But high-level harmonics occur at the output of the regulator, as the input sine wave input form is disturbed because of chopping. So, additional filtering units such as passive filters or coupling transformers have to be used at the output in these AC choppers, in order to eliminate the voltage harmonics. Nowadays there are many studies on switch-mode buck [12, 13], boost [14-17], and buck-boost [18, 19] type AC-AC regulators that are used for direct AC regulation. The mentioned switch-mode AC-AC regulators can achieve output voltages close to sine wave. The harmonic levels of the output voltages are reduced efficiently. So the requirement of additional filtering units is prevented in these types of regulators. Lower complex topology structure of these regulators brings another advantage. Although the application for AC regulation of these switch-mode AC-AC regulators is achieved successfully in the literature, application cases of input AC voltages that are far from sine wave are ignored in these studies. Just only the case of applying pure sine-wave input AC voltage is considered in these similar existing studies in the literature. But in practice, distribution network voltages are disturbed because of nonlinear loads. So AC loads may be supplied with input voltages that are not ideal sine-wave and include voltages harmonics. Thus harmonic elimination in addition to AC voltage regulation is a necessity. This is essential, because the AC loads require supply voltages with low harmonics under 5% THD [20].

A three-phase boost-type active tracking AC-AC voltage regulator is presented in this study. An improved control method is also proposed for the active tracking of the desired output sine-wave phase voltages. The presented control method and the topology of the regulator are patented by the co-author of this study [21]. The presented topology of the regulator incorporates just three capacitors, three inductors, and twelve active switches. This is a moderate number of components. The boost-type structure of the presented regulator enables the achievement of a wide range of output voltage amplitudes for each phase higher than the input phase voltage

amplitudes. Also the modular structure of the regulator topology enables independent control for each output phase operation. Thus supplying of balanced/unbalanced wye-connected three-phase loads or independent single-phase loads by nearly close to ideal sine wave voltages can be achieved by the modularity of the regulator. The proposed control method for the proposed regulator is a novel hybrid control method apart from the similar studies in the literature, it is composed of a closed-loop PID controller and a new feedforward controller. In this way, active tracking of the reference sine-wave output phase voltages is improved to achieve nearly close to sine-wave output phase voltages independent whether the input phase voltages are pure sine-waves or not. Both experimental and simulation test studies are performed for the proposed regulator system. The achieved results for both simulation and experimental tests verify the proposed switch-mode boost-type regulator's ability to provide output phase voltages nearly close to the sine wave with THD values under 5%.

2. THE THREE-PHASE BOOST AC-AC REGULATOR

The proposed boost converter based three-phase AC-AC regulator topology, as well as the regulator's operation procedure and the dynamic analysis, are all discussed in this section.

2.1. The Topology of the Regulator

The proposed boost converter based three-phase AC-AC regulator's main circuit is shown in Figure 1 [21].

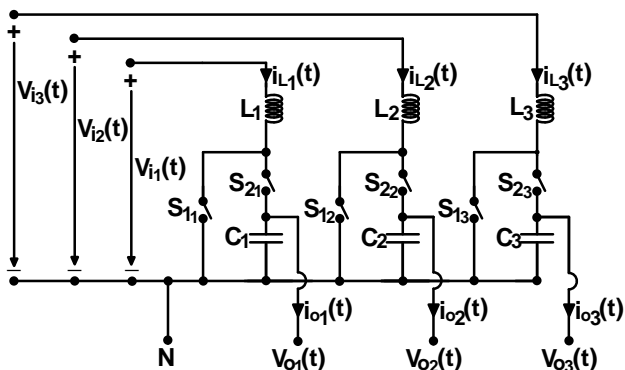


Figure 1 General topology of the proposed boost converter based three-phase AC-AC regulator

The proposed three-phase AC-AC regulator is structured by three boost converter-based sub-circuits, which are wye-connected at the common neutral point (N) as shown in Figure 1. In Figure 1, the “1,2,3” which are the second-order subscripts, mark the three-phase phase number. The mentioned phase number is generalized as “n” where n=1,2,3 in this paper. The neutral point N of the regulator sub-circuits and the three-phase load neutral are connected to provide a neutral return. Thus three-phase unbalanced or three independent single-phase modular regulator operations can also be provided by the proposed regulator structure.

In Figure 1, the input AC phase voltages, the output AC phase voltages, the inductors, and the capacitors are marked by V_{in} , V_{on} , L_n , and C_n , respectively. S_{1n} and S_{2n} represent the bidirectional active switches. IGBTs are used to obtain these bidirectional active switches. Thus the circuit of the proposed regulator, where S_{1n} and S_{2n} are structured by IGBTs, are depicted in Figure 2.

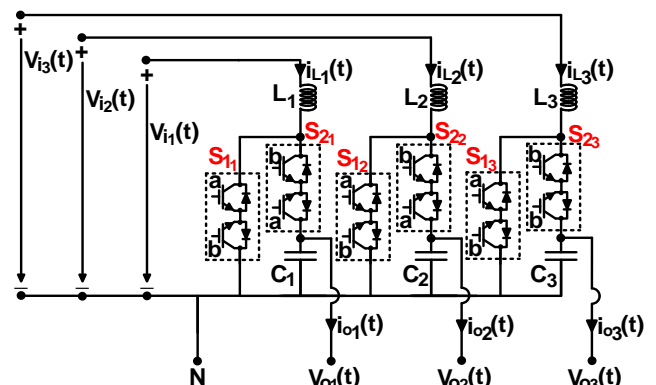


Figure 2 The proposed boost-type three-phase AC-AC regulator circuit with IGBTs

2.2. The Operation Procedure of the Regulator

The proposed three-phase AC-AC regulator's operation is based on the well-known conventional boost converter. The structures of each phase-sub-circuits are taken as identical in this study. The instant input phase voltages $V_{in}(t)$ are boosted as $V_{on}(t)$ phase voltages at the output, based on the PWM duty ratios (d_n) control of S_{1n} . As a result, the output phase voltages are AC voltages of the same polarity as the input phase voltages, but with larger amplitude values. The

S_{2n} switches are the supplementary switches of the S_{1n} switches. S_{2n} are turned off, while S_{1n} are turned on. In this stage the inductors are supplied by V_{in} , and the output phase loads are supplied by the pre-energized capacitors. S_{2n} are turned on, while S_{1n} are turned off. In this stage the output phase loads and the capacitors are supplied by the pre-energized inductors.

As the input phase voltages V_{in} have alternating voltage wave forms, the polarities of V_{in} are forced to be changed in each half period. Thus, the states of the sub-active switches that are part of the bidirectional active switches S_{1n} and S_{2n} must be changed depending on the input phase voltages' half-periods. In Table 1, the control of S_{1n} and S_{2n} active switches are given in detail.

Table 1
Control signal of IGBTs used in Figure 2 as part of the bidirectional S_{1n} and S_{2n} active switches

State	S_{1n}				S_{2n}			
	Positive Half-Wave Stage		Negative Half-Wave Stage		Positive Half-Wave Stage		Negative Half-Wave Stage	
	S_{1an}	S_{1bn}	S_{1an}	S_{1bn}	S_{2an}	S_{2bn}	S_{2an}	S_{2bn}
ON	on	off	off	on	off	on	on	off
OFF	off	off	off	off	off	off	off	off

The switching pattern of the IGBTs can be seen in Figure 3.

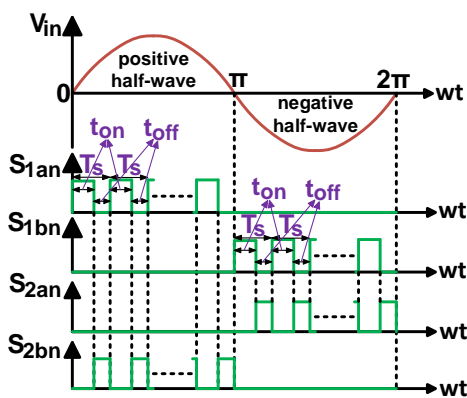


Figure 3 The switching pattern of the IGBTs

Figure 4 gives the proposed regulator topology's equivalent sub-circuits regarding Figure 2 and depending on the control of the active switches for one cycle of the input sine-wave voltage.

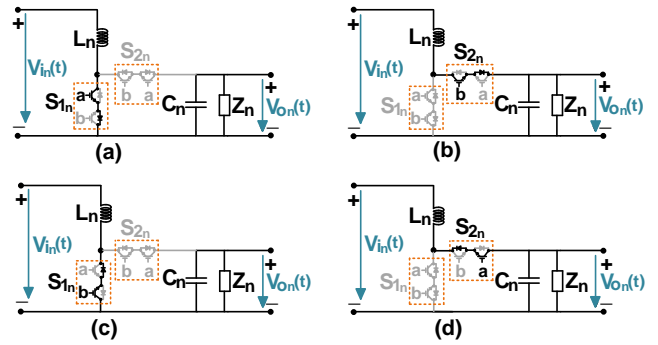


Figure 4 The equivalent sub-circuits of the proposed boost type regulator (a) Positive half-wave output stage, on mode (S_{1n} is on, S_{2n} is off), (b) Positive half-wave output stage, off mode (S_{1n} is off, S_{2n} is on), (c) Negative half-wave output stage, on mode (S_{1n} is on, S_{2n} is off), (d) Negative half-wave output stage, off mode (S_{1n} is off, S_{2n} is on)

So the proposed regulator's one cycle output phase voltage producing operation can be explained as a summary of Figure 3 and Figure 4 for the two main stages as below.

Stage 1 ($0 \leq wt < \pi$): The input AC phase voltages are in positive half-wave periods depending on the determined polarities in this stage. During PWM on-stages of S_{1n} (S_{2n} are off), S_{1an} are turned on, S_{1bn} are turned off and both S_{2an} and S_{2bn} are turned off. During PWM off-stages of S_{1n} (S_{2n} are on), both S_{1an} and S_{1bn} are turned off, S_{2an} are turned off, and S_{2bn} are turned on. From the input phase voltages, the desired positive half sine-waves output phase voltages are produced based on the continuous proper control of d_n , which are the PWM duty ratios of S_{1n} .

Stage 2 ($\pi \leq wt < 2\pi$): The input AC phase voltages are in the negative half-wave periods depending on the determined polarities in this stage. During PWM on-stages of S_{1n} (S_{2n} are off), S_{1bn} are turned on, S_{1an} are turned off and both S_{2an} and S_{2bn} are turned off. During PWM off-stages of S_{1n} (S_{2n} are on), both S_{1an} and S_{1bn} are turned off, S_{2bn} are turned off, and S_{2an} are turned on. From the input phase voltages, the desired negative half sine-waves output phase voltages are produced, based on the continuous proper control of d_n , which are the PWM duty ratios of S_{1n} .

2.3. The Dynamic Analysis of the Regulator

This section presents the dynamic analysis of the proposed boost converter-based three-phase AC-AC regulator in detail. In order to provide an accurate analysis for real-time applications, the analysis takes real parasitic effects of the elements used in the topology into account.

Figure 5 gives the equivalent circuits of the proposed regulator for the positive half-wave input state. The selected IGBTs are considered identical in the equivalent circuit.

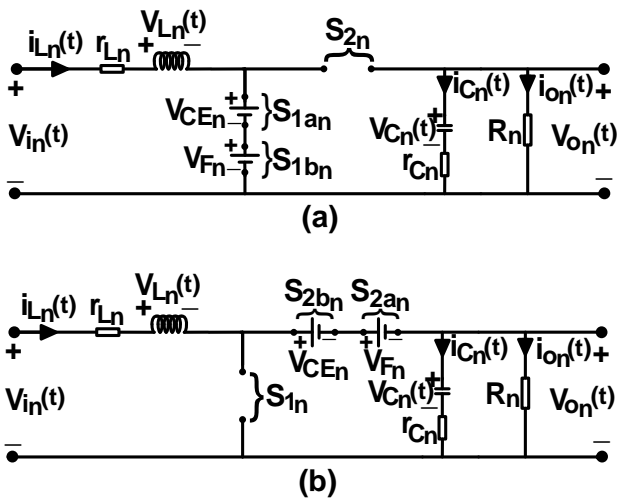


Figure 5 The positive half-wave stage equivalent circuit of the regulator (a) on-mode – S_{1n} is turned on and S_{2n} is turned off, (b) off-mode – S_{1n} is turned off and S_{2n} is turned on

In Figure 5 i_{on} , i_{Ln} , i_{Cn} , V_{Ln} , V_{Cn} , V_{Fn} , V_{CE_n} , r_{Ln} , r_{Cn} , and R_n are the output currents, the inductor currents, the capacitor currents, the inductor voltages, the capacitor voltages, the forward biasing voltages of the IGBTs' anti-parallel diodes, the collector-emitter on-voltages of the IGBTs, the equivalent series resistances (ESRs) of the inductors, the ESRs of the capacitors, and the output phase load resistances, respectively.

The regulator's dynamic analysis can be derived from Figure 5 for the positive half-wave input state. The dynamic equations for the inductor currents and the output voltages are derived for two modes, on-mode and off-mode, as shown in Figure 5.

On-mode (S_{1n} are on and S_{2n} are off): For the on-mode, the state equations of the inductor currents and the output voltages can be achieved according to Figure 5a, respectively as below:

$$\frac{di_{L_n}(t)}{dt} = -\frac{1}{L_n} r_{L_n} i_{L_n}(t) + \frac{1}{L_n} V_{i_n}(t) - \frac{1}{L_n} [V_{CE_n} + V_{F_n}] \quad (1)$$

$$\frac{dV_{o_n}(t)}{dt} = -\frac{1}{(R_n + r_{C_n})C_n} V_{o_n}(t) \quad (2)$$

Off-mode (S_{1n} are off and S_{2n} are on): For the off-mode, the state equations of the inductor currents and the output voltages can be achieved according to Figure 5b, respectively as below:

$$\frac{di_{L_n}(t)}{dt} = -\frac{1}{L_n} r_{L_n} i_{L_n}(t) - \frac{1}{L_n} V_{o_n}(t) + \frac{1}{L_n} V_{i_n}(t) - \frac{1}{L_n} [V_{CE_n} + V_{F_n}] \quad (3)$$

$$\frac{dV_{o_n}(t)}{dt} = \left(\frac{R_n}{R_n + r_{C_n}} \right) \left[\frac{1}{C_n} - \frac{r_{C_n} r_{L_n}}{L_n} \right] i_{L_n}(t) - \left(\frac{R_n}{R_n + r_{C_n}} \right) \left(\frac{r_{C_n}}{L_n} + \frac{1}{R_n C_n} \right) V_{o_n}(t) + \frac{r_{C_n} R_n}{(R_n + r_{C_n}) L_n} V_{i_n}(t) - \frac{r_{C_n} R_n}{(R_n + r_{C_n}) L_n} [V_{CE_n} - V_{F_n}] \quad (4)$$

From (1) and (2), the equations of the state-space model for the on-mode can be derived as follows:

$$\begin{bmatrix} \dot{i}_{L_n}(t) \\ \dot{V}_{o_n}(t) \end{bmatrix} = \begin{bmatrix} -\frac{r_{L_n}}{L_n} & 0 \\ 0 & -\frac{1}{(R_n+r_{C_n})C_n} \end{bmatrix} \begin{bmatrix} i_{L_n}(t) \\ V_{o_n}(t) \end{bmatrix} + \begin{bmatrix} \frac{1}{L_n} & \frac{1}{L_n} & \frac{1}{L_n} \\ 0 & 0 & 0 \end{bmatrix} \begin{bmatrix} V_{i_n}(t) \\ V_{CE_n} \\ V_{F_n} \end{bmatrix} \quad (5)$$

From (3) and (4), the equations of the state-space model for the off-mode can be derived as follows:

$$\begin{bmatrix} \dot{i}_{L_n}(t) \\ \dot{V}_{o_n}(t) \end{bmatrix} = \begin{bmatrix} -\frac{r_{L_n}}{L_n} & -\frac{1}{L_n} \\ \frac{R_n}{R_n+r_{C_n}} \left[\frac{1}{C_n} - \frac{r_{C_n}r_{L_n}}{L_n} \right] & -\frac{R_n}{R_n+r_{C_n}} \left(\frac{r_{C_n}}{L_n} + \frac{1}{R_n C_n} \right) \end{bmatrix} \begin{bmatrix} i_{L_n}(t) \\ V_{o_n}(t) \end{bmatrix} + \begin{bmatrix} \frac{1}{L_n} & \frac{1}{L_n} & \frac{1}{L_n} \\ \left(\frac{R_n}{R_n+r_{C_n}} \frac{r_{C_n}}{L_n} \right) & -\left(\frac{R_n}{R_n+r_{C_n}} \frac{r_{C_n}}{L_n} \right) & -\left(\frac{R_n}{R_n+r_{C_n}} \frac{r_{C_n}}{L_n} \right) \end{bmatrix} \begin{bmatrix} V_{i_n}(t) \\ V_{CE_n} \\ V_{F_n} \end{bmatrix} \quad (6)$$

The above shown dynamic analysis is performed for the positive half-wave input case, as mentioned previously. A similar dynamic analysis for the negative half-wave input case provides the same state-space equations given in (5) and (6). Thus, this means that the state-space equations obtained in (5) and (6) are valid for all input cases.

So, through (5) and (6), the small signal transfer functions between the output phase voltages and the PWM duty ratios can be achieved as follows:

$$G_{boost_n}(s) = \frac{\hat{V}_{o_n}(s)}{\hat{d}_n(s)} = \frac{g_n s + (a_n g_n + c_n f_n)}{s^2 + (a_n + e_n)s + (a_n e_n - b_n c_n)} \quad (7)$$

The coefficients used in (7) are as follows:

$$a_n = \frac{r_{L_n}}{L_n} \quad (8)$$

$$b_n = -\frac{(1-\bar{D}_n)}{L_n} \quad (9)$$

$$c_n = \frac{(1-\bar{D}_n)R_n}{R_n+r_{C_n}} \left[\frac{1}{C_n} - \frac{r_{C_n}r_{L_n}}{L_n} \right] \quad (10)$$

$$e_n = \frac{(1-\bar{D}_n)R_n}{R_n+r_{C_n}} \frac{r_{C_n}}{L_n} + \frac{1}{(R_n+r_{C_n})C_n} \quad (11)$$

$$f_n = \frac{\bar{V}_{o_n}}{L_n} \quad (12)$$

$$g_n = -\frac{R_n}{R_n+r_{C_n}} \left[\frac{1}{C_n} - \frac{r_{C_n}r_{L_n}}{L_n} \right] \bar{i}_{L_n} + \frac{R_n}{R_n+r_{C_n}} \frac{r_{C_n}}{L_n} \left[\bar{V}_{o_n} - \bar{V}_{i_n} + V_{CE_n} + V_{F_n} \right] \quad (13)$$

In (9)-(13), \bar{D}_n , \bar{i}_{L_n} , \bar{V}_{o_n} , and \bar{V}_{i_n} represent the values of PWM duty ratios, inductor currents, output phase voltages, and input phase voltages respectively at the operating point. \bar{V}_{o_n} and \bar{i}_{L_n} can be formulated as below:

$$\bar{V}_{o_n} = \frac{\bar{V}_{i_n}}{(1-\bar{D}_n)}, \quad \bar{i}_{L_n} = \frac{\bar{V}_{i_n}}{(1-\bar{D}_n)R_n} \quad (14)$$

3. THE PROPOSED HYBRID CONTROL METHOD FOR THE REGULATOR OPERATION

The proposed hybrid control method for the control of the proposed AC-AC regulator is presented in this section. Figure 6 demonstrates the general control diagram of the proposed regulator.

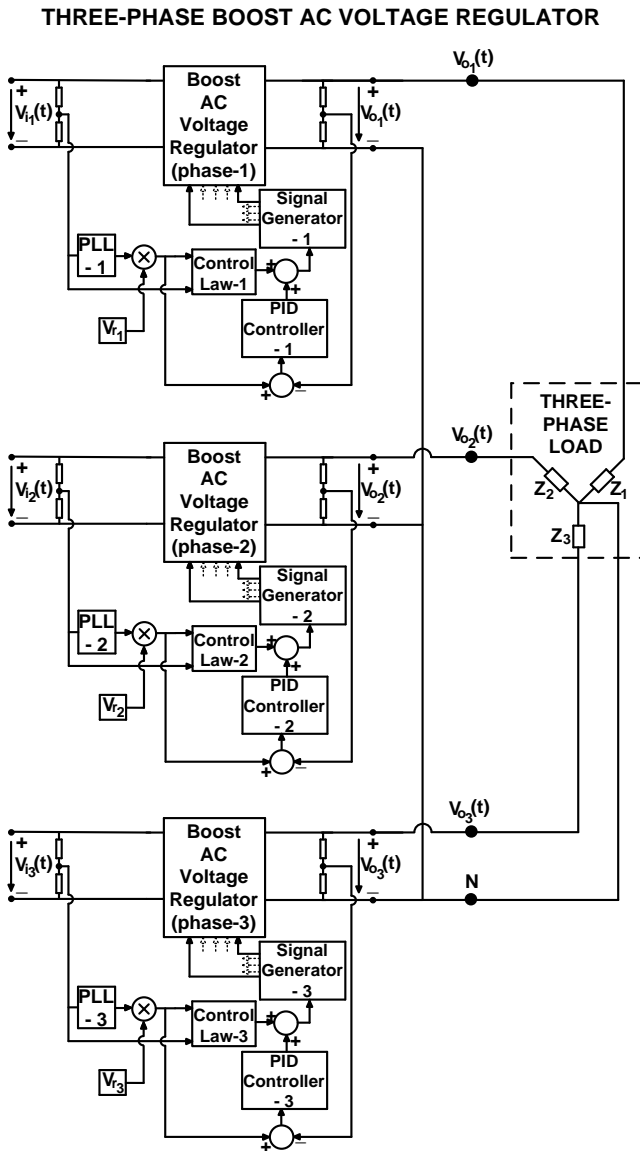


Figure 6 The general control diagram of the proposed regulator

The frequencies of the phase AC voltages of the input are determined by the PLLs, where the magnitudes of the reference output AC phase voltages are determined by V_m as seen in Figure 6. So the requested sine-wave AC reference phase output voltages can be achieved as given below

$$\left. \begin{aligned} V_{ref_1}(wt) &= V_{r_1} \sin w_1 t \\ V_{ref_2}(wt) &= V_{r_2} \sin(w_2 t - 120^\circ) \\ V_{ref_3}(wt) &= V_{r_3} \sin(w_3 t + 120^\circ) \end{aligned} \right\} \quad (15)$$

The proposed hybrid controller is composed of two main units as depicted in Figure 6. One of these units is the traditional closed-loop PID controller. The main mission of the PID controller is to eliminate the error between the real output voltage and the reference output voltage, while it satisfies the response performance depending on the design criteria. The newly developed feedforward controller, which is referred to as “control law (CL)” in Figure 6, is the other unit of the hybrid controller. The developed CL is a controller based on the open-loop, which generates a PWM duty ratio depending on the equation below based on the topology parameters.

$$d_{CL_n}(wt) = \sqrt{\frac{2L_n |V_r \sin w_n t|^2 (|V_r \sin w_n t| - |V_i(wt)| + V_{CE_n} + V_{F_n})}{|V_i(wt)| |V_r \sin w_n t| (|V_i(wt)| - V_{CE_n} - V_{F_n}) T_s R_n}} \quad (16)$$

T_s determines the PWM switching period in (16). The CL’s PWM duty ratio as generated in (16) is not capable of directly meeting the desired PWM duty ratio to obtain the reference output voltage. Instead it generates a duty ratio that is very close to the necessary one. It is clear from (16) that the duty ratio obtained by the CL can be produced in a fast manner as it has a static structure. Thus an improved response performance to obtain the requested duty ratio can be obtained, as the CL supports the PID controller. By this way, accurate and efficient active tracking of the reference output voltage can be provided by the proposed hybrid control method and thus close to sine-wave output voltage with low THD can be obtained with the hybrid control method. So the PID controller and the CL produce the requested PWM as given below:

$$d_n(wt) = d_{PID_n}(wt) + d_{CL_n}(wt) \quad (17)$$

Discrete time control is performed for the regulator operation control in the study. The block diagram of the regulator which is based on the proposed hybrid control method can be given in Figure 7.

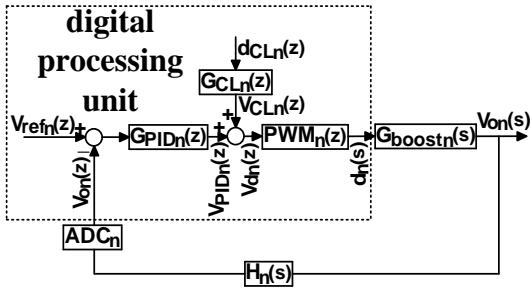


Figure 7 The discrete-time control block diagram based on the proposed hybrid control technique for the boost-type 3-phase regulator

By Figure 7, the fundamental relations between the transfer functions and the control signals of the discrete-time control block diagram are determined as given below.

$$G_{CL_n}(z) = \frac{1}{PWM_n(z)} \quad (18)$$

$$V_{d_n}(z) = V_{CL_n}(z) + V_{PID_n}(z) \quad (19)$$

$$d_n(z) = V_{d_n}(z) \cdot PWM_n(z) \quad (20)$$

The discrete PID controller's transfer function used in this study is given as

$$G_{PID_n}(z) = K_{P_n} + K_{I_n} \frac{z}{z-1} + K_{D_n} \frac{z-1}{z} \quad (21)$$

4. THE STUDY RESULTS

This section gives the design steps of the proposed regulator and also the test results of the simulation and of the experiments.

4.1. The Design Criteria of the Regulator Operation

A laboratory set-up is performed for the proposed regulator for a real-time experimental regulator operation. The set-up is designed for 0-200 Vp input phase voltages (50 Hz), and 0-300 Vp output phase voltages, and 1.8 kW output power. Table 4

IXGH20N60BU1 type n-channel high-speed IGBTs ($V_{CES}=600$ V, $V_{CE}=1.7$ V, $V_F=1.6$ V, $I_C=40$ A) are used in the set-up circuit. In Table 2, the determined values of the inductors, the capacitors and the switching frequencies for the phase sub-units of the regulator circuit are given.

Table 2

The selected values of the switching frequencies, capacitors and inductors

Switching Frequencies f_{sn} (kHz)	Capacitors		Inductors	
	C_n (μF)	r_{Cn} ($m\Omega$)	L_n (μH)	r_{Ln} ($m\Omega$)
50	10	190	50	150

Table 3 determines the operating point parameters of the discrete-time PID controllers for the phase sub-units.

Table 3

The considered operating point parameters of the regulator operation

\bar{V}_{i_n} (V)	\bar{D}_n	\bar{V}_{o_n} (V)	R_n (Ω)
50	0.5	100	40

The parameters of the PID controller used in (21) are found by the design and performance criteria as,

$$K_{P_n} = -0.0082, K_{I_n} = 0.0345, K_{D_n} = 0.014 \quad (22)$$

4.2. The Simulation Results

To validate the theoretical proposals of the study, simulation tests are applied with the proposed hybrid control approach on the proposed regulator.

In MATLAB Simulink, three different simulation test cases are applied to the regulator system, as shown in Table 4. In Figures 8-10, the simulation test results of the wave form are shown. In Table 5, the simulation numerical results of the output are also given. THD_{Vn} and THD_{In} in Table 5 denote the voltages THD and currents THD, respectively.

Table 4
Test cases of the simulation studies

Test Case No	V_{in} (V)			Output Load Z_n			Desired output fundamental sine-wave voltage V_{on} (V)		
	V_{i1}	V_{i2}	V_{i3}	Z_1	Z_2	Z_3	V_{o1}	V_{o2}	V_{o3}
1	50V sine (f=50Hz)	80V sine (f=50Hz)	100V sine (f=50Hz)	Resistive $R_1=25\Omega$	Resistive $R_2=25\Omega$	Resistive $R_3=25\Omega$	160	160	160
2	90V sine + HOH (f=50Hz)	75V sine (f=50Hz)	65V sine + LOH (f=50Hz)	Inductive $R_1=5\Omega, L_1=12mH$	Inductive $R_2=5\Omega, L_2=12mH$	Inductive $R_3=5\Omega, L_3=12mH$	120	120	120
3	70V sine + LOH (f=50Hz)	40V sine + HOH (f=50Hz)	60V sine + fluct. (f=50Hz)	Resistive $R_1=10\Omega$	Inductive $R_2=8\Omega, L_2=6,8mH$	Capacitive $R_3=5\Omega, C_3=0.5mF$	150	110	100

fluct.: fluctuations, HOH: high order harmonics, LOH: low order harmonics

Figures 8-10 and Table 5 prove that the proposed three-phase AC-AC regulator based on the boost-converter can provide the desired AC sine-wave phase voltages close to a sine-wave with under 5% THD levels, though the input AC phase voltages have harmonics or the three-phase output is unbalanced. The results also show that the proposed three-phase AC-AC regulator based on the boost-converter can operate in modular mode for single-phase independent loading. The obtained results given in Figures 8-10 and Table 5 show that the proposed hybrid control method is capable of active tracking of the reference output phase voltages in an accurate and an efficient manner.

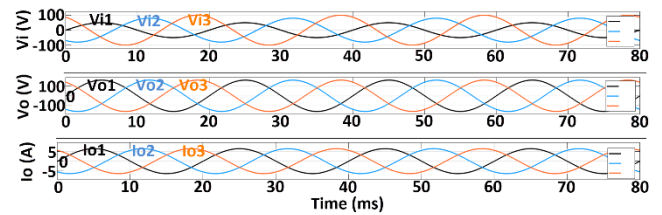


Figure 8 The simulation results for test case-1

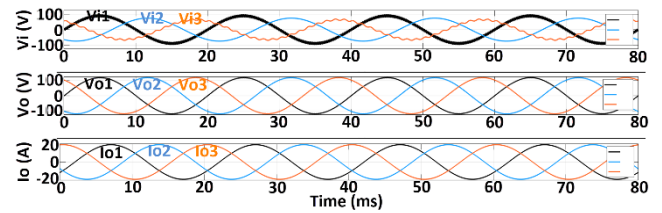


Figure 9 The simulation results for test case-2

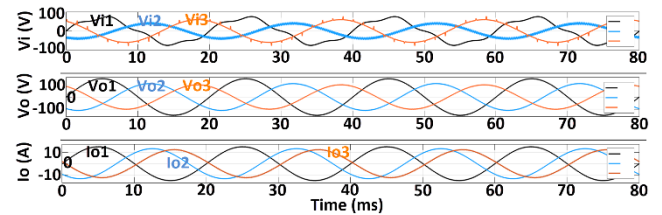


Figure 10 The simulation results for test case-3

Table 5
The numerical simulation results of the test cases

Test Case No	Obtained Fundamental V_{on} (V)			THD V_n (%)			THD I_n (%)		
	V_{o1}	V_{o2}	V_{o3}	THD V_1	THD V_2	THD V_3	THD I_1	THD I_2	THD I_3
1	160.1	160.1	160.1	1.72	1.72	1.72	1.72	1.72	1.72
2	119.8	119.8	119.8	1.93	1.93	1.93	1.76	1.76	1.76
3	150.3	109.9	100.4	1.89	2.13	2.07	1.89	2.02	2.23

4.3. The Experimental Results

To validate the real-time practical application of the study, experimental tests are applied with the proposed hybrid control approach on the proposed regulator. In Figure 11, the experimental set-up of the regulator system which was built for this study is shown.

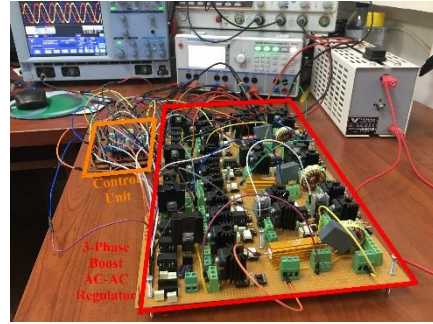


Figure 11 The designed experimental laboratory set-up of the regulator system

Table 6
Test cases of the experimental studies

Test Case No	V_{in} (V)			Output Load Z_n			Desired output fundamental sine-wave voltage V_{on} (V)		
	V_{i1}	V_{i2}	V_{i3}	Z_1	Z_2	Z_3	V_{o1}	V_{o2}	V_{o3}
1	100V sine (f=50Hz)	85V sine (f=50Hz)	55V sine (f=50Hz)	Resistive $R_1=40\Omega$	Resistive $R_2=40\Omega$	Resistive $R_3=40\Omega$	150	150	150
2	25V sine (f=50Hz)	35V sine (f=50Hz)	45V sine (f=50Hz)	Inductive $R_1=9\Omega, L_1=5mH$	Inductive $R_2=9\Omega, L_2=5mH$	Inductive $R_3=9\Omega, L_3=5mH$	75	75	75
3	40V sine (f=50Hz)	40V sine (f=50Hz)	40V sine (f=50Hz)	Resistive $R_1=16\Omega$	Inductive $R_2=7\Omega, L_2=3.3mH$	Capacitive $R_3=20\Omega, C_3=0.33mF$	80	70	90

On the designed laboratory set-up, three different experimental test cases are applied to the regulator system, as shown in Table 6. In Figures 12-14 the experimental wave form test results are shown. In Table 7 the experimental numerical results of the output are also given.

Figures 12-14 and Table 7 prove that the proposed three-phase AC-AC regulator based on the boost-converter can provide the desired AC sine-wave phase voltages close to the sine-wave with under 5% THD levels although the three-phase output is unbalanced. The results also show that the proposed three-phase AC-AC regulator based on the boost-converter can operate in modular mode for single-phase independent loading. Hence, the obtained results given in Figures 8-10 and Table 5 show that the proposed hybrid control method is capable of active tracking of the reference output phase voltages in an accurate and an efficient manner experimentally.

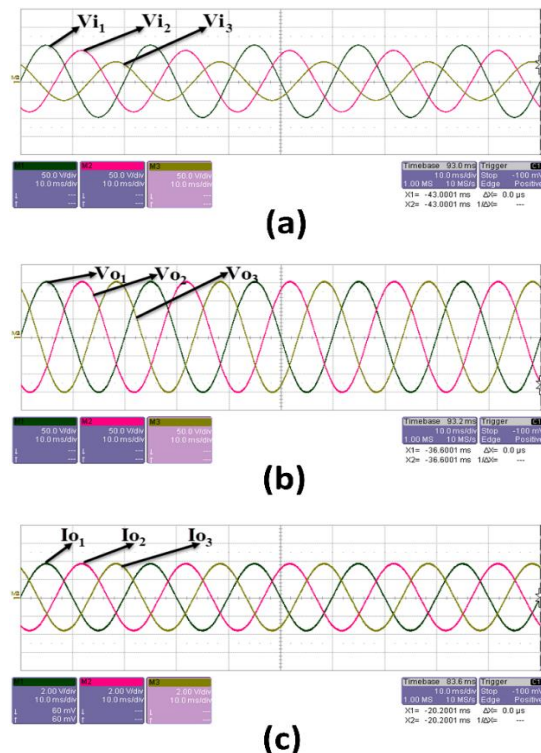


Figure 12 The experimental results for test case-1 (V/div=A/div for I_{on})

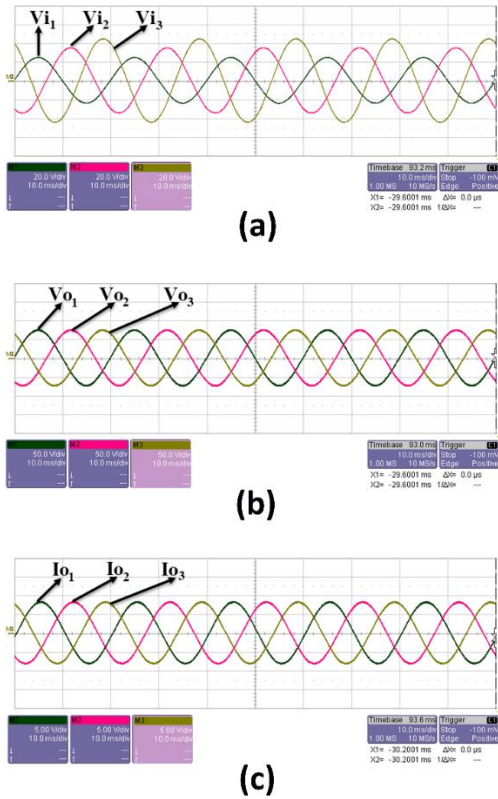


Figure 13 The experimental results for test case-2 (V/div=A/div for I_{on})

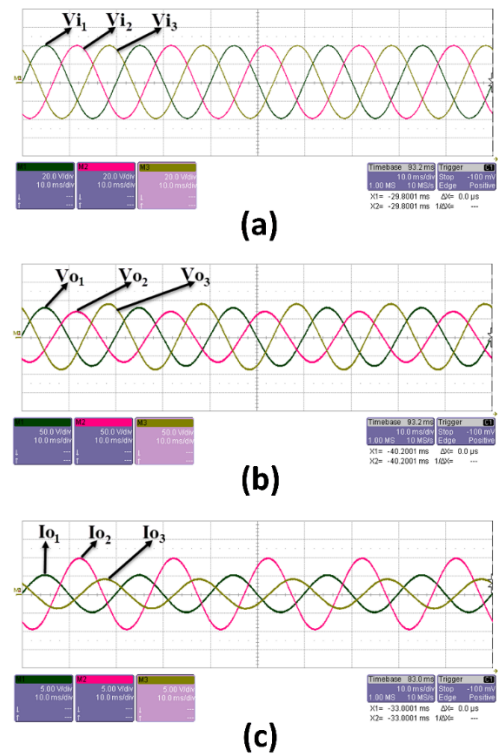


Figure 14 The experimental results for test case-3 (V/div=A/div for I_{on})

Table 7 The achieved numerical experimental results of the test cases

Test Case No	Obtained Fundamental V_{on} (V)			THD $_{Vn}$ (%)			THD $_{In}$ (%)		
	V_{o1}	V_{o2}	V_{o3}	THD $_{V1}$	THD $_{V2}$	THD $_{V3}$	THD $_{I1}$	THD $_{I2}$	THD $_{I3}$
1	150.1	150.3	150.2	1.91	1.94	1.92	1.86	1.89	1.84
2	74.8	74.8	74.9	2.12	2.23	2.09	1.99	2.07	1.94
3	80.4	70.2	89.9	1.86	2.07	1.99	1.81	1.90	2.18

Table 8 Comparative THD results for the proposed hybrid control and the standalone traditional PID control of the experimental test cases

Test Case No	THD (%) results of the proposed hybrid control method						THD (%) results of the traditional standalone PID control					
	THD $_{Vn}$			THD $_{In}$			THD $_{Vn}$			THD $_{In}$		
1	1.91	1.94	1.92	1.86	1.89	1.84	1.98	2.08	2.05	1.93	1.99	1.94
2	2.12	2.23	2.09	1.99	2.07	1.94	2.23	2.31	2.21	2.12	2.17	2.09
3	1.86	2.07	1.99	1.81	1.90	2.18	1.97	2.21	2.10	1.92	1.98	2.27

A comparative test study is done to show the proposed hybrid control technique’s efficiency on the active tracking. The proposed hybrid control technique and the standalone PID control are applied separately to the proposed regulator for the comparative test case parameters as $V_{i2}=50V$ sine, $V_{o2}=110V$, $R_2=10\Omega$. In Figure 15 the

obtained output voltage waveforms of phase-2 for the mentioned two separate applications are demonstrated together. In Table 8 the comparative numerical output THD results of these applications are also presented.

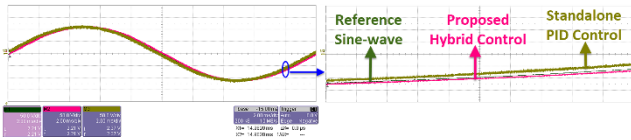


Figure 15 Comparative experimental wave forms for the output phase-2 voltage V_{o2} of the proposed hybrid control and of the standalone PID control for $V_{i2}=50\text{V}$ sine, $V_{o2}=110\text{V}$, $R_2=10\Omega$ (50V/div, 2ms/div)

It is clear from Figure 15 that the proposed hybrid control technique provides better active tracking of the reference phase output sine-wave voltages than the traditional PID control. Thus, it is proved that the developed CL is capable of improving the active tracking by supporting the PID controller. The output THD results in Table 8 also prove this. It must be noted that in Table 8 the THD results are under 5%.

The proposed boost converter based three-phase regulator's efficiency is researched for different output power rates depending on the power rate determined in the design criteria. The obtained efficiency curve of the regulator is demonstrated in Figure 16. As seen from Figure 16, the proposed regulator efficiency is sufficient.

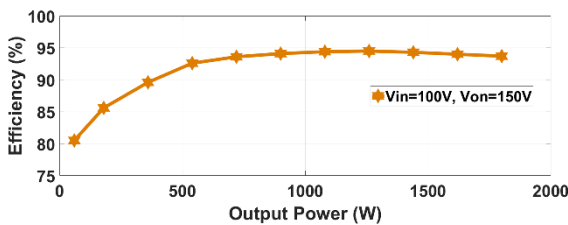


Figure 16 The regulator's efficiency curve for different output power rates

5. CONCLUSION

This study proposes a boost converter-based three-phase active tracking AC-AC voltage regulator operating in switch-mode. The proposed regulator topology includes a moderate number of active and passive elements. A new feedforward controller supports the closed-loop PID controller. This robust hybrid control method is proposed for the regulator operation control. By this hybrid control, the response of the active tracking for the reference output phase voltages is increased and provides close to sine-wave output

phase voltages, whether the input AC phase voltages are ideal pure sine or not. The modular regulator topology structure also enables independent control of each output phase operation that provides the supply of balanced/unbalanced wye-connected three-phase loads or independent single-phase loads with close to ideal sine-wave voltages. Both experimental and simulation test studies are done for the proposed three-phase AC regulator to demonstrate the accuracy and the efficiency of the proposals. The achieved results show that the proposed regulator with the proposed hybrid control method provides accurate and efficient operation for producing output phase voltages nearly close to sine-wave THD values under 5% for different regulator operation parameters.

Acknowledgments

The topology and the control theory of the proposed AC regulator in the study are patented by the co-author in Austrian Patent Office as "Aktive Netzfilter" (patent no: AT 505460 B1, filed 10.07.2007, applied 15.06.2012).

Funding

The authors received no financial support for research and publication of this article.

The Declaration of Conflict of Interest/ Common Interest

No conflict of interest or common interest has been declared by the authors.

Authors' Contribution

The authors contributed equally to the study.

The Declaration of Ethics Committee Approval

The authors declare that this document does not require an ethics committee approval or any special permission.

The Declaration of Research and Publication Ethics

The authors of the paper declare that they comply with the scientific, ethical and quotation rules of SAUJS in all processes of the paper and that they do not make any falsification on the data collected. In addition, they declare that Sakarya University Journal of Science and its editorial board have no responsibility for any ethical violations that may be encountered, and that this study has not been evaluated in any academic publication environment other than Sakarya University Journal of Science.

REFERENCES

A sample references list is given below;

- [1] S. Subramanian and M. K. Mishra, "Interphase AC-AC topology for voltage sag supporter," *IEEE Transactions on Power Electronics*, vol. 25, no. 2, pp. 514–518, 2010.
- [2] D. M. Lee, T. G. Habetler, R. G. Harley, T. L. Keister, and J. R. Rostron, "A voltage sag supporter utilizing a PWM-switched autotransformer," *IEEE Transactions on Power Electronics*, vol. 22, no. 2, pp. 626–635, 2007.
- [3] K. Yamamoto, Y. Tsurusaki, S. Ehira, and M. Ikeda, "Suppression of compensation voltage pulsations for voltage sag/swell compensator utilizing single-phase matrix converter," 2015 18th International Conference on Electrical Machines and Systems, pp. 581–586, 2015.
- [4] K. Yamamoto, S. Ehira, and M. Ikeda, "Synchronous frame control for voltage sag/swell compensator utilizing single-phase matrix converter," *IEEJ Journal of Industry Applications*, vol. 6, no. 6, pp. 353–361, 2017.
- [5] L. R. Merchan-Villalba, J. M. Lozano-García, J. G. Avina-Cervantes, H. J. Estrada-García, A. Pizano-Martínez, and C. A. Carreno-Meneses, "Linearly decoupled control of a dynamic voltage restorer without energy storage," *Mathematics*, vol. 8, no. 10, article number: 1794, 2020.
- [6] A. H. Soomro, A. S. Larik, M. A. Mahar, A. A. Sahito, and I. A. Sohu, "Simulation-based analysis of a dynamic voltage restorer under different voltage sags with the utilization of a PI controller," *Engineering Technology & Applied Science Research*, vol. 10, no. 4, pp. 5889–5895, 2020.
- [7] K. Mikolajuk and A. Tobola, "Piecewise signals for the iterative control of the voltage conditioner," 2019 IEEE 20th International Conference on Computational Problems of Electrical Engineering, pp. 154–157, 2019.
- [8] H. Hafezi, R. Faranda, and M. C. Falvo, "Single-phase dynamic voltage conditioner control under load variation," *Proceedings of 2016 17th International Conference on Harmonics and Quality of Power*, pp. 563–568, 2016.
- [9] T. Shahsavarian, Y. Cao, E. Anagnostou, and R. Kalbfleisch, "Novel modulated equivalent model of point-to-point LCC-based high voltage AC/DC/AC system for geomagnetic storm-induced unbalanced harmonic studies," *International Journal of Electrical Power & Energy Systems*, vol. 122, article number: 106173, 2020.
- [10] A. E. L. Da Costa, N. Rocha, C. B. Jacobina, and E. L. L. Fabricio, "Single-phase AC-DC-AC three-level three-leg converter with reduced switch count," *IEEE Transactions on Power Electronics*, vol. 35, no. 3, pp. 2295–2307, 2020.
- [11] B. Triyono, M. Y. Fauzan, Soedibyo, and M. Ashari, "Filter design of PWM AC chopper on soft starting application 3 phase induction motors," 2016 1st International Seminar on Application for Technology of Information and Communication: Science and Technology for a Better Future, pp. 285–289, 2016.

- [12] U. A. Khan, A. A. Khan, H. Cha, H. G. Kim, J. Kim, and J. W. Baek, "Dual-buck AC-AC converter with inverting and non-inverting operations," *IEEE Transactions on Power Electronics*, vol. 33, no. 11, pp. 9432–9443, 2018.
- [13] J. G. Wang and R. McMahon, "Highly reliable and efficient voltage optimizer based on direct PWM AC-AC buck converter," *IEEE Transactions on Energy Conversion*, vol. 35, no. 4, pp. 1897–1906, 2020.
- [14] A. Kumar, R. Raman, D. Sarkar, P. K. Sadhu, and A. Banerjee, "Improvement in performance of induction heating system using direct AC-AC boost converter," 2018 2nd International Conference on Power, Energy and Environment: Towards Smart Technology, 2018.
- [15] H. Sarnago, O. Lucia, A. Mediano, and J. M. Burdio, "Direct AC-AC resonant boost converter for efficient domestic induction heating applications," *IEEE Transactions on Power Electronics*, vol. 29, no. 3, pp. 1128–1139, 2014.
- [16] A. A. Khan, H. Cha, and H. F. Ahmed, "High efficiency buck and boost type AC-AC converters," 2015 17th European Conference on Power Electronics and Applications, 2015.
- [17] A. Chakraborty, A. Chakrabarti, and P. K. Sadhu, "Analysis of a full-bridge direct AC-AC boost converter based domestic induction heater," *Revue Roumaine Des Sciences Techniques - Serie Electrotechnique Et Energetique*, vol. 64, no. 3, pp. 223–228, 2019.
- [18] H. F. Ahmed, M. S. El Moursi, H. Y. Cha, K. Al Hosani, and B. Zahawi, "A reliable single-phase bipolar buck-boost direct PWM AC-AC converter with continuous input/output currents," *IEEE Transactions on Industrial Electronics*, vol. 67, no. 12, pp. 10253–10265, 2020.
- [19] M. Zhou, Y. Sun, M. Su, X. Li, F. L. Liu, and Y. L. Liu, "A single-phase buck-boost AC-AC converter with three legs," *Journal of Electrical Engineering & Technology*, vol. 13, no. 2, pp. 838–848, 2018.
- [20] F. Yalcin, "A novel buck converter based three-phase inverter with feedforward supported closed-loop control," *Electric Power Components and Systems*, vol. 48, no. 14-15, pp. 1445–1463, 2020.
- [21] F. Himmelstoss, "Aktive Netzfilter," Austrian Patent, patent no: AT 505460 B1, filed 10 July 2007, applied 15 January 2012.